geoconvention
Calgary • Canada • May 11-13 2026

AVA modelling with VTI Zoeppritz including Q

Scott Leaney, Evan Mutual, Raul Cova, Bill Goodway
Qeye

Summary

The primaries-only convolutional forward model for equal-angle or amplitude-versus-angle (AVA) gathers remains a common approach in AVO/AVA inversion wherein it is standard practice to use a linearized, small-contrast approximation. The VTI version of this approach makes use of Ruger's extension to small-contrast isotropic reflection coefficients. The inclusion of Q contrasts in AVA inversion has received relatively little attention. We consider primaries-only convolutional AVA modelling but make use of exact VTI Zoeppritz reflection coefficients and include Q anisotropy. Including Q may be important in cases such as viscous oil sands with very low Q or to distinguish gas from oil. We review some aspects of the theory and show a synthetic example based on field logs.

Theory

Zoeppritz reflection coefficient routines do not take as input an incidence angle but rather the horizontal slowness or ray parameter, p_1 (in addition to medium properties above and below the interface). In isotropic media the ray parameter is given by $p_1 = \sin(\theta)/c$, where θ is the ray angle from interface-normal (e.g. vertical) and c is the velocity of the medium. In the anisotropic case, θ is the phase angle and the velocity is now the phase velocity at angle θ. Considering VTI or polar anisotropy, given the unit phase direction, $(\hat{p}_1, \hat{p}_3) = (\sin\theta, \cos\theta)$, the ray parameter is given by $p_1 = \hat{p}_1/c$, where the P-wave phase velocity is given in terms of density-normalized stiffness moduli, $A_{ij} = C_{ij}/\rho$, by (Chapman, 2004, 5.7.34)

$$c^2 = \frac{1}{2}\left(A_{55} + A_{33}\hat{p}_3^2 + A_{11}\hat{p}_1^2 + \sqrt{\left((A_{33} - A_{55})\hat{p}_3^2 - (A_{11} - A_{55})\hat{p}_1^2\right)^2 + 4\hat{p}_3^2\hat{p}_1^2 a^2}\right) \quad (1)$$

with $a = A_{13} + A_{55}$.

We will be making use of a Zoeppritz routine for VTI media based on the approach of Schoenberg and Protazio (1992), first utilized for plane-wave modelling (Folstad and Schoenberg, 1992). We include Q in this Zoeppritz routine by making the stiffness moduli complex with the imaginary component defined according to $C_{ij}^I = C_{ij}^R/Q_{ij}$ (e.g. Carcione and Cavellini, 1994). We note that while others have defined frequency-dependent stiffnesses via a relaxation function or explicit dispersion relation, here we consider frequency-independent moduli as was done extensively by Zhu and Tsvankin (2006).

We have explored different approaches to defining the VTI Q-matrix, Q_{ij}; here we describe our use of the eigenstiffness method (Mehrabadi and Cowin, 1990; Chapman, 2021). The eigenstiffness approach requires four Q values for VTI media, three associated with shear: Q_1, Q_2, Q_3, and one for dilatational (P) waves, Q_4. The three shear Q values are associated with axial directions $Q_1 = Q_{Sv} = Q_{55}$, $Q_2 = Q_{Sh} = Q_{66}$ and another for propagation near 45 degrees, Q_3. We

assign axial (vertical) Q_P and Q_S values, or those corresponding to the entries in the Q-matrix, Q_{33} and Q_{55}. We say $Q_{66} = Q_{55}(1 + 2\gamma)$, an approach also taken by Xi and Yin (2024). We amplify Q_{Sv} by an anellipticity factor to get the off-axis eigenstiffness shear Q, $Q_3 = Q_1(1 + A)$, where A is Schoenberg's anellipticity parameter (Schoenberg et al., 1996) and use an eigenstiffness equation to back-calculate Q_4 such that $Q_{33} = Q_P$. Given these four eigenstiffness Q values a set of equations provides the complex stiffnesses, C_{ij}, in terms of the real stiffnesses, C_{ij}^R, and hence the Q-matrix is defined (Chapman, 2021).

The angle-dependence of effective P-wave Q may be computed from the complex phase velocity -squared (Carcione and Cavellini, 1994; Carcione, 1997) by using equation (1) with complex moduli. The directional Q value is then obtained as the ratio of the real/imaginary parts of c^2. We note that we are considering only a real phase slowness vector presently. The complex case, known as inhomogeneous ray theory, is an area for future research.

Results

To investigate properties using the theory described above we consider VTI media with Q (VTIQ) across an interface and then AVA synthetics based on field log data. The upper half-space medium has VTIQ parameters: $(V_p, V_s, \varepsilon, \delta, \gamma, Q_p, Q_s) = (2.16, 0.80, 2.25, 0.19, 0.06, 0.31, 50, 30)$. This produces a Q-matrix with entries $(Q_{11}, Q_{13}, Q_{33}, Q_{55}, Q_{66}) = (57, 67, 50, 30, 49)$. For interface AVA modelling we use a lower halfspace (reservoir) medium with VTIQ parameters: $(V_p, V_s, \varepsilon, \delta, \gamma, Q_p, Q_s) = (2.47, 1.12, 2.16, 0.04, 0.01, 0.06, 5, 3)$. The Q-matrix for the reservoir lower half space is $(Q_{11}, Q_{13}, Q_{33}, Q_{55}, Q_{66}) = (3.0, 2.3, 3.0, 5.0, 5.6)$. Note that $Q_p < Q_s$, consistent with measurements (Gautam et al., 2003: Batzle et al., 2005) for partially saturated porous media. The effective medium Q_p and Q_s values were obtained by volume averaging $1/Q$ for matrix and a water-bitumen mixture given PHIE and Sw. Figure 1 shows effective Q_p versus angle for upper and lower half spaces. Note the difference in vertical scales and relatively larger variation in the upper medium due to stronger anisotropy.

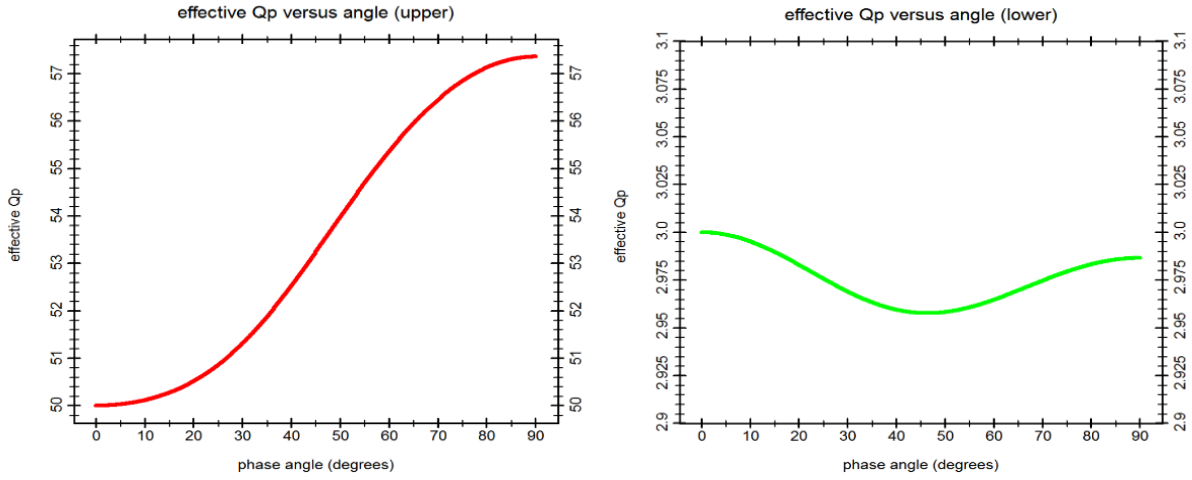


Figure 1. Effective Qp versus angle for the upper medium (left) and the lower medium (right). Note the difference in vertical scales.

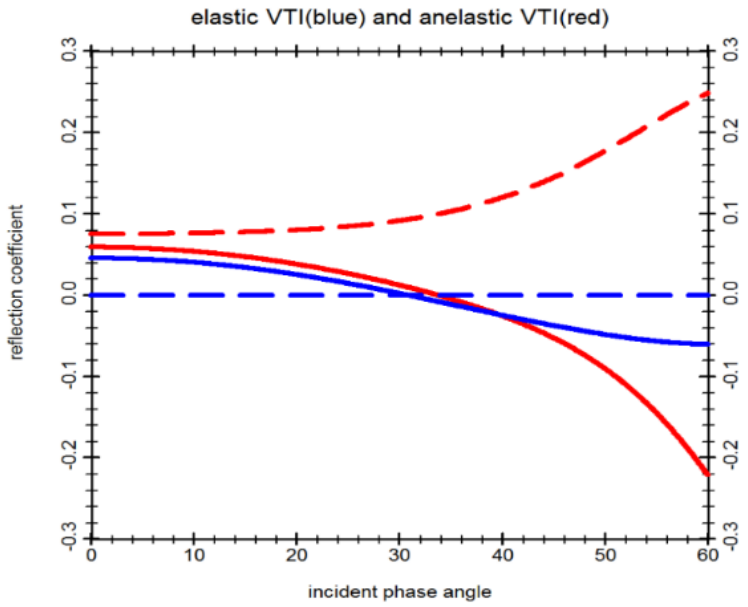


Figure 2. Elastic VTI P-p reflection coefficients (blue) and anelastic coefficients (red). Real (solid) and imaginary (dashed) components are shown.

Figure 2 shows VTI and VTIQ P-p reflection coefficients versus incident phase angle. Note the increase in the real part of the reflection coefficient at small-to-moderate angles and the significant imaginary component of the VTIQ coefficients at all angles, indicating a phase rotation that increases with angle.

The AVA synthetics make use of field logs from an oil sands well. The VTI properties were assigned using a semi-empirical approach involving Vshale and porosity (Leaney and Hornby, 2025). Continuous logs of Qp and Qs were assigned using the aforementioned volume averaging approach with shale and reservoir sand end-members. A more sophisticated rock physics model including anelastic clay in anisotropic shale (Sayers, 2025) may be considered in future work. The anelastic VTI logs were converted to time at a sample interval of 0.1ms and then upscaled and resampled to 0.5ms. The wavelet used was Ormsby with corner frequencies (3,8,200,300) Hz. Complex convolution was done in the frequency domain to capture phase rotation due to imaginary reflection coefficients from Q and/or post-criticality.

The AVA synthetics in Figure 3 show incident phase angles out to 40 degrees for VTIQ and VTI cases. The observed differences over the reservoir indicate that the effect of Q may be observable in field data. This shows that it may be advantageous to include Q as a facies attribute in a VTI+Q probabilistic AVA inversion as it should help to discriminate low-Q viscous oil sand facies where impedance contrasts are small, or to discriminate low-Q gas from oil.

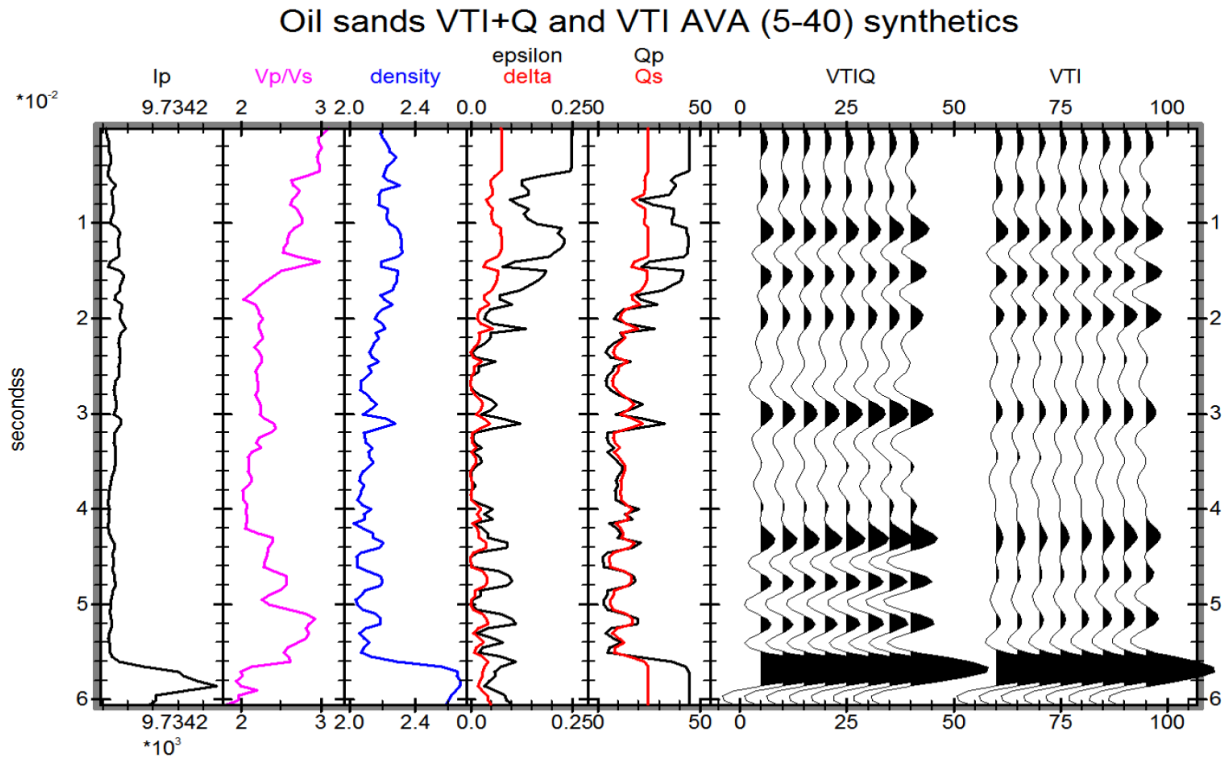


Figure 3. VTIQ logs: Ip, Vp/Vs, density, epsilon, delta, Qp, Qs with VTI+Q and VTI AVA synthetics out to 40 degrees incident phase angle.

Conclusions

Viscous oil sands with low impedance contrast and gas-versus-oil scenarios may benefit from the inclusion of Q in reflection coefficients and AVA inversion. We considered exact VTI Zoeppritz reflection coefficients and included Q by making the VTI moduli complex. Upper half-space horizontal slowness input to VTIQ Zoeppritz uses the VTI phase velocity. We adapted the eigenstiffness approach to define the Q matrix corresponding to the Voigt stiffness moduli. Interface reflection coefficients were computed for an upper half-space shale and a lower half-space reservoir medium with low Q values. An increase was found in the real part of the reflection coefficient at small angles with a significant imaginary part at all angles, indicating a phase rotation increasing with incidence angle. Synthetic AVA gathers based on field logs from an oil sands well indicate that a Q effect may be observable in field prestack seismic data. This forward modelling work shows that Q may be useful to include in a seismic facies parameter vector and inversion to help distinguish low-Q pore-space fill, whether heavy oil or gas.

Acknowledgements

Many thanks as always to Chris Chapman for theoretical tutelage.

References

Batzle, M., Hofmann, R., Prasad, M., Gautam, K., Duranti, L. and Han, D., 2005, Seismic attenutation: Observations and mechanisms: *75th Annual International Meeting, SEG, Expanded Abstracts*, 1565–1568.

Carcione, J.M. and Cavallini, F., 1994. A rheological model for anelastic anisotropic media with applications to seismic wave propagation: *Geophys. J. Int.*, **119**, 338-348.

Carcione, J.M., 1997, Reflection and transmission of qP-qS plane waves at a plane boundary between viscoelastic transversely isotropic media: *Geophys. J. Int.*, **129**, 669-680.

Chapman, C.H., 2004, *Fundamentals of seismic wave propagation*, Cambridge University Press.

Chapman, C.H., 2021, “TI attenuation”, SLB internal note.

Folstad, P.G. and Schoenberg, M., 1992, Low-frequency propagation through fine layering: *SEG Expanded Abstracts*, 1249-1251.

Gautam, K., Batzle, M. and Hofmann, R., 2003, Effect of fluids on attenuation of elastic waves: *73rd Annual International Meeting, SEG, Expanded Abstracts*, 1592–1595.

Leaney, S. and Hornby, B., 2025, Deviated well sonic logs, anisotropy and AVA: *Geoconvention*.

Mehrabadi, M.M. and Cowin, S.C., 1990. Eigentensors of linear anisotropic elastic materials: *Q. J. Mech. appl. Math.*, **43**, 15-41.

Sayers, C.M., 2025, Elastic attenuation and dispersion anisotropy of clay in shales: *Geophysics*, **91**, No. 1, 1-11.

Schoenberg, M. and Protazio, J., 1992, ‘Zoeppritz’ rationalized and generalized to anisotropy, *Journal of Seismic Exploration*, **1**, 125-144.

Schoenberg, M., Muir, F. and Sayers, C., 1996, Introducing ANNIE: A simple three-parameters anisotropic velocity model for shales: *Journal of Seismic Exploration*, **5**, 35-49.

Xi, Y. and Yin, X., 2024, Characterization and analysis of attenuation anisotropy in viscoelastic vertical transverse isotropic media: *Geophysical Prospecting*, **72**, 1831-1851.

Zhu, Y. and Tsvankin, I., 2006, Plane-wave propagation in attenuative transversely isotropic media: *Geophysics*, **71**, No. 2, T17-T30.